frontiers | Frontiers in Environmental Chemistry

TYPE Original Research
PUBLISHED 17 March 2025
DOI 10.3389/fenvc.2025.1552966

OPEN ACCESS

EDITED BY
David Amouroux,
UMR5254 Institut des Sciences Analytiques et de Physico-Chimie pour l'Environnement et les Matériaux (IPREM), France

REVIEWED BY
Juan Carlos Nóvoa-Muñoz,
University of Vigo, Spain
Svetoslava Todorova,
Syracuse University, United States

*CORRESPONDENCE
V. F. Taylor,
vivien.f.taylor@dartmouth.edu

RECEIVED 29 December 2024
ACCEPTED 26 February 2025
PUBLISHED 17 March 2025

CITATION
Goss P, Landis JD, Wang T and Taylor VF (2025) Atmospheric and river-derived mercury fluxes in distinct natural communities of a river delta. *Front. Environ. Chem.* 6:1552966. doi: 10.3389/fenvc.2025.1552966

Atmospheric and river-derived mercury fluxes in distinct natural communities of a river delta

P. Goss, J. D. Landis, T. Wang and V. F. Taylor*

Department of Earth Science, Dartmouth College, Hanover, NH, United States

Introduction: River deltas play an important role in sequestering and storing mercury (Hg), restricting its release into downstream bodies of water. Delta landscapes encompass a patchwork of distinct wetland soils and vegetation, which accumulate Hg from both atmospheric and watersheds sources, and have varying capacities for long-term Hg retention.

Methods: To better understand Hg retention in the complex mosaic of delta soils, this study used soil age models based on fallout radionuclides (FRNs, ^{210}Pb, ^{7}Be, ^{241}Am) to measure Hg flux to three distinct natural communities in the Missisquoi River Delta, Vermont.

Results: Soil profiles of radionuclide and Hg flux from a pitch pine bog, a silver maple floodplain forest, and a wild rice marsh all revealed long-term retention of Hg, despite varying susceptibilities to frequent hydrological disturbances. A mass balance approach was applied to apportion Hg fluxes to each region of the delta based on regional values of Hg wet deposition, measured FRN and Hg inventories, and measured or estimated foliar Hg inputs. Spaghnum peat soils of the pitch pine bog had the lowest Hg flux, consistent with uptake predominantly from wet deposition, while Hg accumulation doubled in bog soils developed under shrub or tree canopies, due to strong foliar and non-foliar uptake of gaseous elemental Hg (GEM). Soils in the silver maple floodplain received the highest Hg flux, driven by both GEM uptake and large riverine sedimentary inputs. Surprisingly, submerged soils in the wild rice marsh recorded substantially lower Hg flux than the adjacent silver maple forest, with low inputs of Hg from both GEM and watershed sources.

Conclusion: This novel chronometry framework for elucidating pathways of Hg accumulation across distinct deltaic environments revealed the variable roles of vegetation type and flooding regime in controlling Hg inputs to delta soils.

KEYWORDS

mercury, river delta, soil, flux, apportionment

1 Introduction

River deltas are the interface between rivers and their receiving bodies of water, making them critical regions for watershed mercury (Hg) cycling. Delta soils can capture Hg, a potent neurotoxin, and restrict its release to downstream aquatic ecosystems where it otherwise can bioaccumulate and biomagnify through aquatic food chains (Driscoll et al., 2007). While soils are recognized as major global reservoirs of Hg due to their efficient capture of gaseous elemental mercury (GEM) from the atmosphere (Landis et al., 2024b; Obrist et al., 2018), delta soils are unique in that they also accumulate Hg from watershed

inputs in the form of dissolved and particulate load from their rivers, in addition to atmospheric wet and dry deposition (Liu et al., 2022; Wang et al., 2004; Zhang et al., 2015). The balance of riverine and atmospheric sources in determining delta Hg storage remains unclear. While deltas are complex landscapes formed from river inputs of fine alluvial silts, clays, and associated organic matter which are likely to supply particulate-bound Hg from the connected upstream watershed (Shanley and Chalmers, 2012), they also produce new organic matter through primary productivity of diverse plant communities with varying potential for GEM uptake (Rydberg et al., 2015). Across these landscapes, variations in wetting/drying regimes, flood recurrence intervals, and degrees of organic horizon development may also impact the degree to which soils accumulate and retain Hg. Evaluating the pathways by which delta soils across different regions of the landscape capture Hg, and the degree to which they retain Hg longterm, are important to understanding their role in buffering aquatic ecosystems from Hg deposition.

Delta wetland environments are a patchwork of landforms and natural communities, which sequester Hg from two distinct sources, i) direct atmospheric deposition, termed wet deposition if by precipitation, and dry depostion through sorption and foliar uptake of GEM by vegetation, and ii) river inputs of dissolved and particle-bound Hg derived from watershed soils, sediments, and vegetation (Driscoll et al., 2007). Recent efforts to evaluate Hg accumulation in soils have revealed the critical role of overlying vegetation, and particularly dense forest canopies, which efficiently sequester GEM directly from the atmosphere (Demers et al., 2015; Jiskra et al., 2015; Landis et al., 2024a; Obrist et al., 2021; Zhou et al., 2023). Plants take up Hg via both stomatal and non-stomatal uptake, which is then passed to the soil via leaf litter, or washed off plant surfaces with precipitation as throughfall (Yuan et al., 2023; Yuan et al., 2021). Direct deposition of GEM to the soil or forest floor surface is also significant and in some cases is the largest source of Hg to soil systems (Obrist et al., 2021; Zhou et al., 2023). Deltas incorporate regions of floodplain forests, wetland plants and peat bogs, which are therefore expected to play a dominant role in mediating atmospheric Hg sequestration.

River inputs of particle-bound Hg to delta soils, derived from watershed soils, sediments, and vegetation, likely vary with flooding regime and proximity to the river channel. Previous studies of the spatial distribution of Hg in delta soils provide a valuable framework for identifying regions in the delta landscape where Hg is stored (Liu et al., 2022; Wang et al., 2004; Zhang et al., 2015), yet these studies are based on measures of Hg concentrations, which are strongly influenced by both soil bulk density and the duration of soil exposure to Hg accumulation and therefore do not yield insights into fluxes or Hg sources. Understanding the processes and pathways by which delta soils capture Hg therefore requires direct measurement of rates of Hg accumulation so that these can be apportioned to different sources and processes.

New approaches to understanding Hg accumulation pathways in soils have focused on forested regions due to their importance to global GEM cycling (Demers et al., 2013; Jiskra et al., 2015; Landis et al., 2024a; Obrist et al., 2021; Yuan et al., 2023; Yuan et al., 2021; Yuan et al., 2019). One recent approach used fallout radionuclides (^{7}Be, ^{210}Pb, ^{137}Cs, ^{241}Am) to directly measure Hg accumulation rates in soils, and by comparison with atmospheric fluxes measured in precipitation, litterfall, and GEM as assessed by a micrometeorological flux gradient approach, quantify the retention of Hg using a mass balance approach (Landis et al., 2024a; 2024b). It is estimated, for example, that forests accumulate Hg at five times the rate of lake sediments due to uptake of GEM, whereas lakes receive primarly wet deposition and are poor receptors for GEM (Landis et al., 2024b). This approach leverages the new LRC age model which is based on the fallout radionuclide ^{210}Pb (half-life 22.3 years) but also incorporates ^{7}Be (half-life 54 days) to correct for penetration of atmospherically derived metals below the soil surface during deposition (non-ideal deposition). This enables the extension of ^{210}Pb chronometric dating to soils and sediments where conditions typically violate foundational assumptions of previous models which require ideal deposition and steady-state (Landis et al., 2016). The LRC model has been established in stable reference locations where the potential for soil disturbance or lateral transfer of organic matter and associated metals is minimized, but its application to dynamic locations such as river deltas has not yet been evaluated.

In this work, we combine FRN chronometry and mass balance to assess the inputs of Hg to river delta soils and to quantify the effect that different delta environments have on Hg storage. We contrast Hg accumulation rates in soils across different regions of the Missisquoi River Delta, in the northeast corner of Lake Champlain, Vermont. We aimed to apportion Hg fluxes across distinct natural communities in three environments of the delta: a Pitch Pine bog, a Silver Maple floodplain forest, and a Wild Rice marsh, having varying flooding frequency, soil organic matter content, and dominant vegetation type. Finally, the study seeks to assess the retention of Hg by a river delta over decadal to centennial time scales.

2 Materials and methods

2.1 Sample collection

Delta soils were sampled in September 2023, November 2023, and April 2024 at the Missisquoi National Wildlife Refuge in northern Vermont, United States. Figure 1 provides a local site map where soils were sampled, while illustrating the complexity of vegetation and land use types.

Soil and overlying vegetation in three distinct natural communities were sampled to capture different hydrologic regimes, soil types and overlying vegetation, which are described in Table 1. Samples were collected from three different subsites of a Pitch Pine Bog (with different overlying vegetation), a Silver Maple Floodplain and a Wild Rice Marsh.

2.2 Pitch pine bog

The Pitch Pine Bog has dominant canopy of *Pinus rigida* which occurs in isolated groves that occur atop islands of accumulated organic matter. The canopy is underlain by *Spaghnum* peat, which dominates in hollows, and an impenetrable understory of huckleberry (*Galussacia baccata*) and mountain holly (*Ilex mucronata*) shrubs on hummocks. The soils are Histosol, ranging

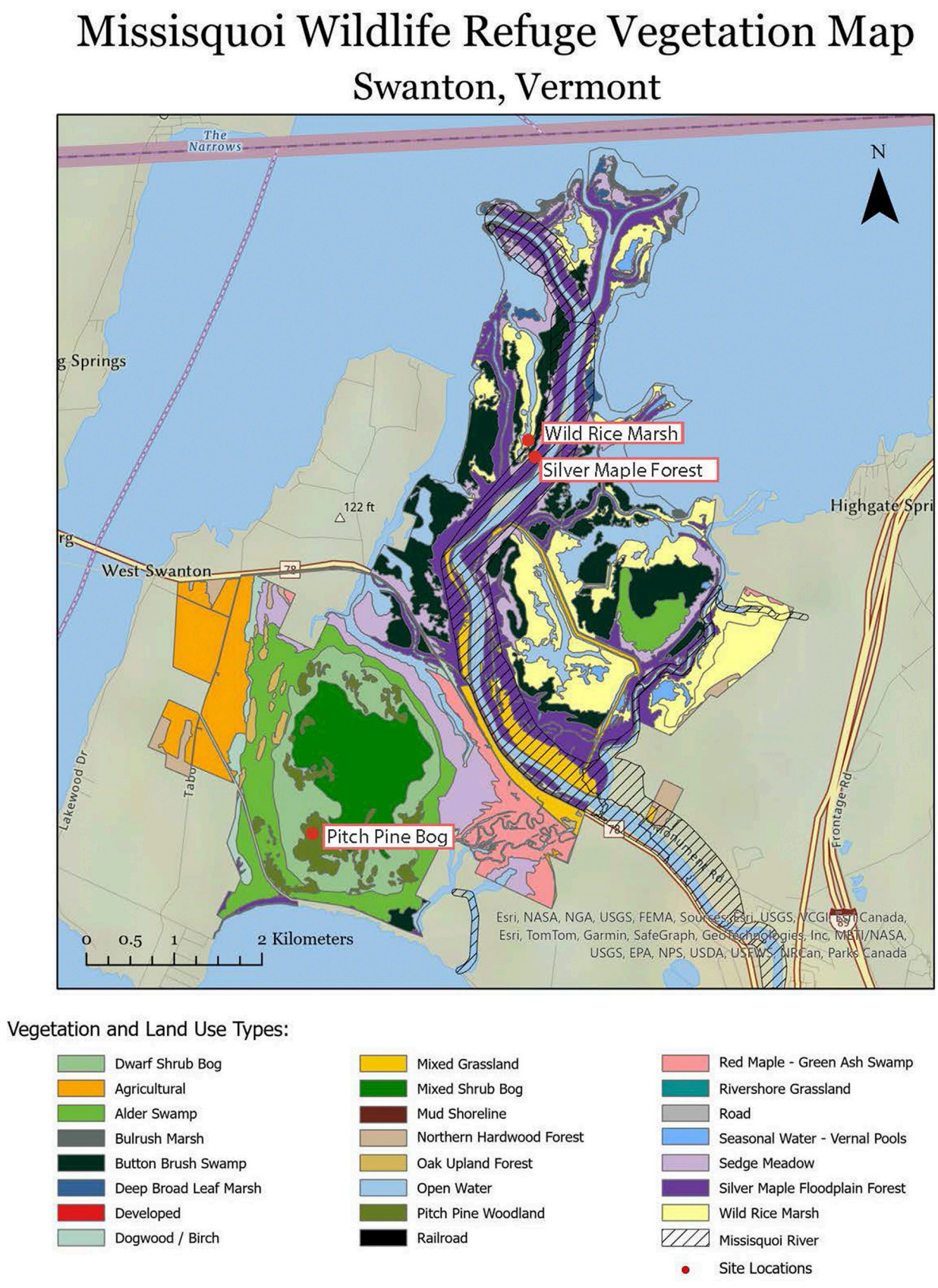

FIGURE 1
Map of vegetation and land use types in the Missisquoi Reservoir, with site locations marked with red circles (adapted from Clews, 2002).

TABLE 1 Vegetation, soil type and flooding frequency of the three environments sampled in the Missisquoi Wildlife Refuge.

Sample site	Vegetation Description	Soil Type	Flooding Regime
Pitch Pine Woodland Bog	Pitch pine woodland bog communities. Sphagnum moss, with dense low shrubs and pitch pine stands	Sphagnum peat and Carlisle muck; deep, poorly drained organic material	Submergence rare
Wild Rice Marsh	Wild rice plants in permanently saturated wetlands	Entisol (Aquent)	Always submerged, 30–60 cm standing water
Silver Maple Forest	Gallery forests dominated by silver maples with green ash, and cottonwood trees. Tall, erect trees with dense canopy	Inceptisol (Aquept)	Annual flooding in spring, high flow events

from folistic under pitch pine and shrubs to hemistic in hollows dominated by *Sphagnum*. To capture the influence of differences in overlying vegetation on Hg inputs, three pits/cores were taken from Pitch Pine Bog. A *Spaghnum* peat core was extracted using a 4-inch diameter 3 ft-long PVC pipe from a hollow which was fully submerged at time of sampling. Two quantitative soil pits (30 × 30 cm area) were excavated under the huckleberry shrub and pitch pine forest communities. Vegetation samples, including overlying shrub leaves and twigs, and pitch pine needles, were collected from a prescribed 50 × 50 cm area above the pits. High resolution quantitative soil pits are described in detail in Landis et al. (2024b). For the Huckleberry pit, samples were collected at 4 cm depth intervals, until ~40 cm, where the water table was reached. For the Pitch Pine pit, samples were collected at 2 cm depth increments from 1 to 16 cm, followed by 4 cm intervals until water table was reached at 32 cm depth. Deeper samples down to 80 cm depth were then obtained from the pitch pine soil by driving a PVC pipe through the pit floor, while using a Silkey 30 cm handsaw to clear roots from the dense network that underlies the pitch pine and huckleberry hummucks. The soil-filled PVC was carefully excavated, capped at depth, and kept vertical to minimize disturbance during transport to the laboratory.

2.3 Silver maple forest

Mature silver maples (*Acer saccharinum*) form high (>30 m) canopies on elevated berms above the Missisquoi River channel. The soils are aquic Inceptisol (Aquept) characterized by strong redoximorphic features through the top 50 cm. Two quantitative soil pits were sampled beneath mature silver maple forest at times of leaf off (April and November). At the times of sampling the water table was encountered at 28 cm (November 2023) and 46 cm (April 2024). Leaf litter samples (Oi horizon) were collected from a 50 × 50 cm area above each pit. Soil pits were 30 × 30 cm, and soil layers were systematically collected and bagged at 1 cm intervals down to a 10 cm depth, then depth intervals were increased to 2 cm then 5 cm, reaching a final depth of 50 cm.

2.4 Wild rice marsh

The Long Channel marsh is an abandoned distributary channel now isolated from the Missisquoi river and Lake Champlain, except at flood stages. Wild rice (*Zizania palustris*) grows on submerged soils in shallow water. The soils are wet Entisol (Aquent), lacking any horizon development and weak accumulation of organic matter. Soil/sediment cores in the wild rice marsh were obtained with a PVC pipe as above. The PVC was hammered into the wild rice bed that was submerged under ~30 cm of water to a sediment depth of ~32 cm before being excavated and capped on either side. Rice stalks and roots were also collected from within a 50 × 50 cm area of the marsh. Samples were then transported back to Dartmouth College with the cores being kept vertical and intact with overlying water as they were transported. In the laboratory, cores were drained of lake water by drilling holes at the standing water level, then the PVC pipe was split and soil samples were sectioned in 2 cm intervals.

All soil and vegetation samples were weighed upon return to the laboratory, then dried at 60°C and reweighed to obtain constant weight. Vegetation samples were homogenized in a stainless-steel Wiley Mini-Mill (Thomas Scientific), and soil samples by agate mortar and pestle or zirconia ball mill.

2.5 Gamma spectrometry

Aliquots of each dry sample were packed and weighed into 110 cm^3 polyethylene pucks for gamma counting, following the methods outlined by Landis et al., 2016. Peaks of ^{210}Pb, ^{137}Cs activity were integrated at characteristic decay energies: ^{7}Be at 477 keV, with correction for ^{228}Ac at 478 keV; ^{210}Pb at 46.6 keV; ^{241}Am at 59.5 keV; ^{137}Cs at 662 keV (from the decay of ^{137m}Ba), and ^{226}Ra at 186 keV. The atmospheric ^{210}Pb component or $^{210}Pb_{ex}$ was calculated as total ^{210}Pb minus supported ^{210}Pb; the latter was estimated by the constant ^{210}Pb/^{226}Ra ratio at depth in each core. Samples were counted for 2–7 days to ensure adequate precision for ^{137}Cs, ^{241}Am, ^{7}Be at the tail of its depth distribution, and ^{226}Ra in defining the 'excess' ^{210}Pb. Calibration of the gamma instruments was conducted using uranium BL5 and thorium OKA2 ores from the Canadian Certified Reference Material Project (CCRMP, NRC Canada, Ottawa). These ores were diluted into matrix soils and sediments similar to our samples. Correction for self-attenuation of gamma emissions from both standards and samples was applied at all energies using a planar multi-nuclide source (Landis et al., 2012).

2.6 ^{210}Pb and ^{7}Be chronometry

The Linked Radionuclide accumulation model (LRC) (Landis et al., 2016) was implemented to establish age-depth models for each soil core. In soil systems, observations of the short-lived radioisotope ^{7}Be reveal that atmospheric elements penetrate the soil medium to

depths beyond the surface; this phenomenon is termed "non-ideal deposition." Penetration typically follows an exponential profile and up to 5% of new deposition can reach soil depths of 10 cm (Landis et al., 2024a). To account for non-ideal deposition in both soil and sediment age models, concurrent measurements of ^{7}Be can be used to quantify the penetration of atmospheric metals, including ^{210}Pb, into the soil subsurface during deposition, provided that geochemical behaviors of the metals are concordant. LRC dating is corroborated using the bomb pulse in ^{241}Am and ^{137}Cs (Landis et al., 2016; Landis et al., 2024). These bomb-derived radionuclides are expected to have the same profile in soils based on their shared source history in atmospheric bomb testing. While ^{241}Am has ~50 times lower abundance, its low biogeochemically mobility make it a more reliable tracer than ^{137}Cs which is prone to being remobilized or biologically cycled as a potassium analog due to its active uptake in plants, e.g., (Kaste et al., 2021; Landis et al., 2016).

2.7 Hg analysis

Aliquots of soils were ground in a zirconia ball mill prior to Hg analysis by Direct Mercury Analyzer (DMA, Milestone). Aliquots (70 mg) of ground soils were weighed into nickel boats and loaded on the DMA. The precision and accuracy of the method was determined by duplicate samples (RPD = 5% ± 5%), and analysis of two standard reference materials (NIST coal, Hg = 90 ng/g, recovery = 95 ± 2%; and NIST New Jersey soil, Hg = 132.9 ng/g, recovery = 107 ± 5%). Fluxes of Hg (μg m^{-2} y^{-1}) to soils were calculated by multiplying the measured Hg concentration (ng g^{-1}) by the mass depth of the soil interval (kg m^{-2}), then dividing by the age difference of the bounding top and bottom layer (y) derived from the LRC model.

2.8 Total inventories

Total soil inventories of $^{210}Pb_{ex}$, ^{241}Am, ^{137}Cs and ^{7}Be were calculated as the sum of activities (Bq m^{-2}) for all depth intervals throughout each core. These are directly comparable to inventories predicted from known rates of atmospheric deposition. Representative ^{210}Pb inventories for lakes receiving primarily wet deposition are 4,440 Bq m^{-2} (Perry et al., 2005), whereas higher reference inventories for soils of ca. 5,200 Bq m^{-2} reflect both wet and dry deposition to forest canopies (Landis et al., 2016; Landis et al., 2024b). Inventories that are higher than those predicted from atmospheric deposition can be used to infer that lateral inputs of particle bound metals are accumulating in the soil core, whereas inventories lower than the predicted ones are interpreted as a lateral loss or erosion of soil-bound metals from the core.

2.9 Loss on Ignition (LOI)

Loss on Ignition (%LOI) was determined as a proxy for soil organic carbon content. Aliquots (0.5 g) of each soil sample were weighed into pre-weighed crucibles, and heated to 550°C degrees for 4 h, cooled to room temperature, then reweighed.

2.10 Geogenic Hg correction

Atmospherically-derived Hg in soils was distinguished from geogenic Hg using aluminum (Al) as a reference element. Geogenic refers to Hg sourced from soil parent material. Aliquots of soil (0.25 g) for Al and major/trace element analysis, were microwave digested in a mixed acid solution (HNO_3-HCl-HF-H_2O_2) then transferred to Teflon vessels and evaporated on a hot plate. Analysis of major and trace elements was conducted using Inductively Coupled Plasma Optical Emission Spectrometry (ICPOES, Spectro ARCOS). The geogenic fraction of Hg was only determined for the primary cores from the Silver Maple forest and Wild Rice marsh soils; the Pitch Pine bog cores were purely organic in composition (~97% LOI) with no mineral parent material and therefore assumed to have negligible geogenic Hg.

Geogenic Hg was calculated as follows: $Hg_{geo} = Al_i \times (Hg_{total}/Al)_{deep}$. The mineral/pre-anthropogenic fraction of Hg was estimated using the aluminum (Al):Hg ratio in deep pre-industrial soils at the base of the core; this ratio was multiplied by the measured concentration of Al in each soil layer to estimate geogenic Hg. Flux of anthropogenic Hg, from atmospheric deposition and the watershed, was then estimated by subtraction of the mineral Hg fraction, $Hg_{anth} = Hg_{total} - Hg_{geo}$. The geogenic correction does not distinguish pre-anthropogenic atmospheric Hg and thus Hg_{anth} reports an anthropogenic atmospheric component in excess of natural atmospheric Hg loading.

3 Results

3.1 Radionuclide profiles and soil age models

Specific activities of $^{210}Pb_{ex}$, ^{7}Be, ^{137}Cs and ^{241}Am were examined relative to cumulative mass depth for each soil core across the three sites, with ground depth also shown on the secondary y-axis; depth profiles of primary cores are given in Figure 2 and data for all cores is in Supplementary Table S1. For all sites, $^{210}Pb_{ex}$ activity decreased exponentially with depth, indicating activity profiles were primarily driven by radioactive decay and therefore suitable for reconstructing soil ages. Penetration of ^{7}Be was evident in the surface of all cores, enabling calculation of the ^{7}Be:$^{210}Pb_{ex}$ ratio which is the basis of the LRC age model.

Across sites in the Pitch Pine Bog, only the Peat could be cored deep enough to reliably capture the entire $^{210}Pb_{ex}$ profile (Supplementary Table S1). For Pitch Pine, we extrapolate from a well-defined exponential decay profile and estimate to have captured 90% of the total Pb inventory, but for Huckleberry only an estimated 40% was recovered above water table (Supplementary Figure S1). LRC age models for all sites were evaluated by corroboration with the bomb pulse radionuclides, ^{241}Am and ^{137}Cs (Figure 2). In the Peat core, the full bomb pulse of both ^{137}Cs and ^{241}Am was present as a broadened band centered at 22 cm. The ^{241}Am peak maximum aligned with a soil age of 1958, in reasonable agreement with the expected bomb pulse of 1963, confirming this core provides a good record of atmospheric deposition. The Pitch Pine and Huckleberry could not be corroborated because full bomb-pulse peaks were not recovered above water table. In both the Silver Maple forest and Wild Rice marsh soils, in contrast to the Peat core, the bomb pulse

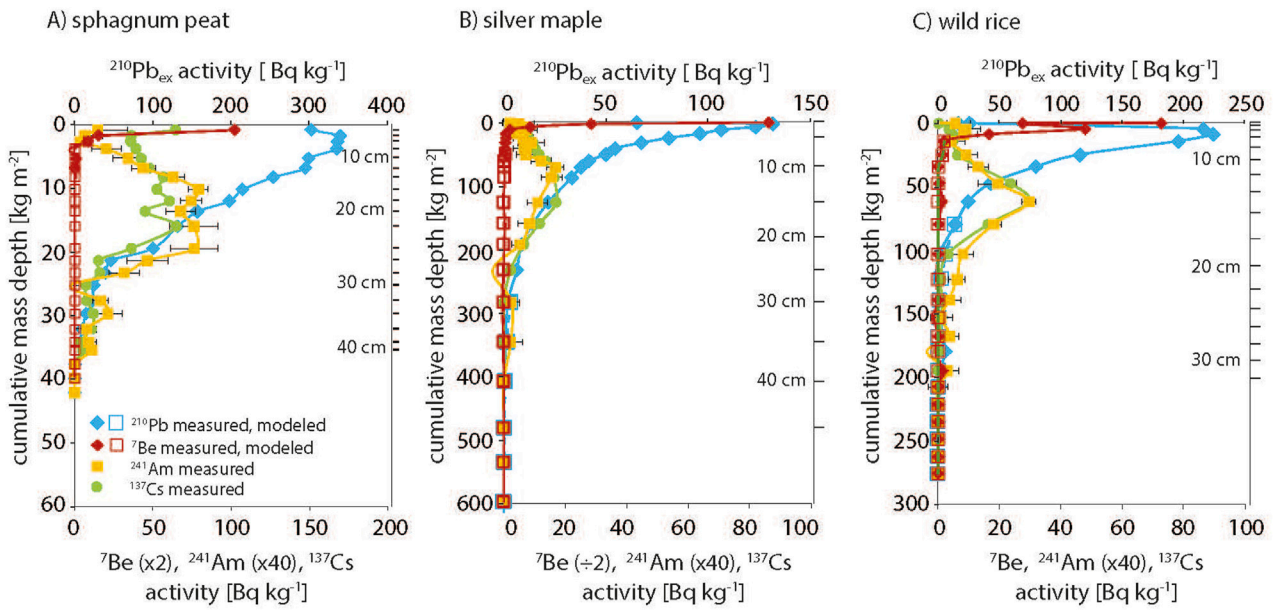

FIGURE 2
Activities of fallout radionuclides (^{7}Be, $^{210}Pb_{ex}$, ^{241}Am, ^{137}Cs) versus cumulative mass depth in the **(A)** Peat core from the Pitch Pine Bog, and primary soil cores from **(B)** the Silver Maple floodplain and **(C)** the Wild Rice marsh. Ground depths are also shown.

TABLE 2 Inventories of radionuclides^{210}Pb,^{241}Am and^{137}Cs for each core. Relative uncertainties are shown for duplicate pits. Inventories of anthropogenic Hg from 1850 to 2024 are also shown (for primary cores only).

Core	$^{210}Pb_{ex}$ (Bq m^{-2})	^{241}Am (Bq m^{-2})	^{137}Cs (Bq m^{-2})	Hg_{anth} (mg m^{-2})
Wild Rice (n = 2)	6,989 ± 9.9	44 ± 6.8	1,434 ± 10	5.28
Silver Maple (n = 2)	7,506 ± 1.1	53 ± 13	2,372 ± 5.8	19.6
Pitch Pine	~8,100	>20	>952	>5
Peat	4,342	34	1,047	4.25
lake inventory[a]	4,400	28	500	3
soil inventory[b]	5,200	32	1,650	8.1

[a]Perry et al. (2005) for 210Pb$_{ex}$, Taylor et al. (2022) for 241Am, 137Cs.
[b]Landis et al. (2016), Landis et al. (2024a).

elements were present as sharp peaks. In the Silver Maple pits, bomb pulse peaks at disparate depth of 20 cm and 12 cm aligned with LRC dates of 1960 and 1978, which for the primary pit, was in good agreement with the known date of 1963; in the secondary pit the maxima was younger than the known date. The bomb pulse peaks in the two Wild Rice cores were clear and sharp at similar depths of 13 and 15 cm, but corresponding dates of 1945 and 1947 were significantly older than the expected age. We suggest that the Wild Rice marsh was likely impacted by major hydrologic disturbance within the past 100 years, which would result in the ^{210}Pb inventory likely being less than steady-state (which requires ~200 years without disturbance) and causing the bomb-pulse to be biased too old. For this case for the purpose of reconstructing Hg fluxes we implemented an alternate age model by assuming a constant mass sedimentation rate based on the observed depth of the ^{241}Am bomb peak and assuming a peak year of 1964 (Supplementary Figure S2).

Radionuclide (^{210}Pb, ^{241}Am and ^{137}Cs) inventories in each core were assessed relative to regional measures of atmospheric deposition (Table 2), to evaluate the amount of lateral movement of particle-bound radionuclides into or away from the core location (Lamborg et al., 2002; Landis et al., 2016). For the Pitch Pine bog, a full inventory was only captured for the Peat core, where ^{210}Pb and ^{241}Am inventories were similar to those expected from direct atmospheric deposition alone. For the Pitch Pine forest core, the recovered ^{210}Pb inventory exceeds expectation for atmospheric deposition. For the Silver Maple forest and Wild Rice marsh cores, ^{210}Pb, ^{241}Am and ^{137}Cs inventories greatly exceeded fluxes expected from atmospheric deposition,. Inventories from duplicate pits in both Wild Rice and Silver Maple show excellent agreement, with differences typically less than 10% (Table 2).

The comparison of peat cores with soils is important to evaluate the suitability of these records for Hg flux

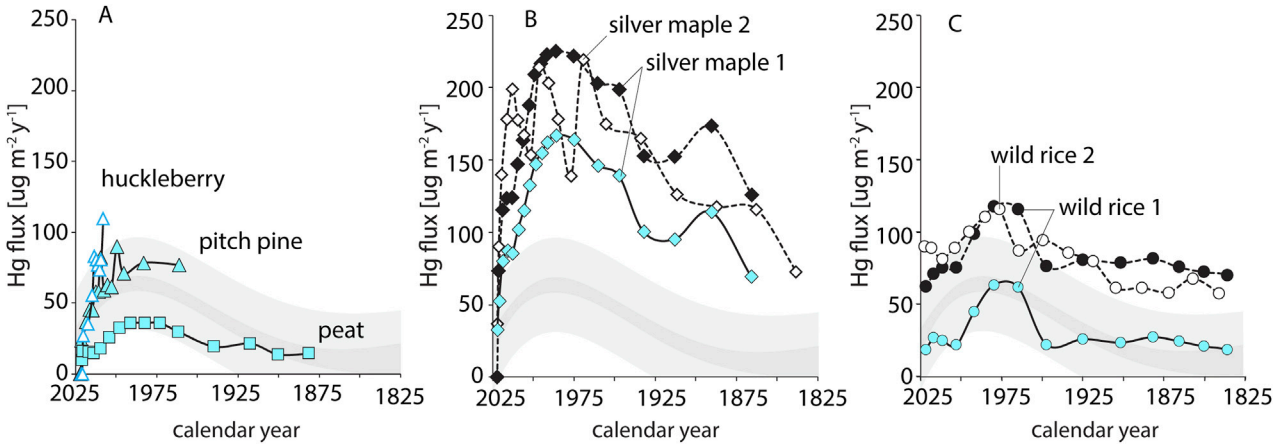

FIGURE 3
Hg flux (μg $m^{-2}y^{-1}$) versus calendar year in **(A)** Pitch Pine bog, **(B)** Silver Maple forest, and **(C)** Wild Rice marsh. Grey bands represent the mean Hg flux (dark grey) and uncertainty of prediction (light grey) to forest soils in the Northeast (bands = 2σ, n = 8 sites) (Landis et al., 2024a). Blue symbols represent flux of anthropogenic Hg_{anth}, black/white symbols represent total Hg flux uncorrected for geogenic/natural atmospheric Hg.

reconstruction. Here, the ^{241}Am peak is broadened in the Peat core (Figure 2), yet the peak maximum (1967) is nonetheless in good agreement with the expected bomb pulse year of 1963. The $^{210}Pb_{ex}$ and ^{241}Am flux inventories for the Peat core (4,300 and 34 Bq m^{-2}, respectively) were also similar to regional values of $^{210}Pb_{ex}$ wet deposition (Landis et al., 2016; Perry et al., 2005), suggesting that peak broadening is due to dispersion within the peat profile rather than net lateral transport of radionuclides into or out of the sampled location.

3.2 Parent material, mercury concentration and flux

%LOI was determined in all soils (Supplementary Table S1). For the two soils and peat from the Pitch Pine bog, %LOI was 95%–98%, indicating nearly pure organic content and negligible mineral content of these soils, whereas for Silver Maple, %LOI ranged from ~32% in the organic surface layers to ~4% in the deeper mineral horizons. In the Wild Rice soils, % LOI was also higher in the surface layers ~27%, and 5%–12% lower in the core. High mineral content in the Long Channel soils is attributable to the alluvial silts that form the parent material of both Silver Maple and Wild Rice soils.

Concentrations of Hg in soils were determined and plotted against cumulative mass depth and ground depth showing the location of the water table (Supplementary Figure S3); Hg flux versus calendar year was then assessed across each soil profile (Figure 3). Reconstructions of Hg flux (Figure 3) were compared with reference fluxes from other northeastern soils (Landis et al., 2024a). Soils in the Silver Maple forest and Wild Rice marsh are shown as total Hg and anthropogenic Hg flux (corrected for geogenic Hg, which was negligible in the highly organic Pitch Pine soils). Notably, all Hg flux profiles follow the shape of those from regional forest soils, peaking in 1975–1990 and declining to present day. Inventories of Hg from the year 1850 to present were calculated for each core (Table 2).

4 Discussion

4.1 River delta soils as archives of deposition history

Across the three sites in the Missisquoi river delta, the soil parent material as well as the delivery pathways of radionuclides and Hg vary, likely due to differences in hydrologic regime, and in their associated natural communities. The ability of these soils to record depositional histories, despite the dynamic hydrology of delta environments, is evidenced in both exponential ^{210}Pb declines and well-defined bomb pulse peaks that are consistent with other regional reference sites (Supplementary Figure S4). While LRC age reconstructions typically have uncertainties better than 10% for reference soils (Landis et al., 2024a), larger errors of ca. 20% observed here based on bomb-pulse peaks reflect the more complex soil processes and histories in the delta environment.

Across all Missisquoi delta sites, reconstructed Hg flux are consistent, increasing histories show consistent histories of Hg flux, increasing due to industrialization in the mid-1850s, and declining in 1970s and 80s until current day following air pollution legislation (Figure 3) (Landis et al., 2024a; Perry et al., 2005; Roberts et al., 2021; Taylor et al., 2022). However, while flux profiles of Hg were similar among the three Missisquoi sites, their magnitudes span nearly a factor of five in total anthropogenic Hg inputs. Lowest flux peaked at 36 μg $m^{-2}y^{-1}$ in the Peat core. Accumulation rates of Hg in the Huckleberry and Pitch Pine soils peak at 70–100 μg $m^{-2}y^{-1}$ which are consistent with other northeastern forest soils (73 ± 5 μg $m^{-2}y^{-1}$; Landis et al., 2024a), although we note that these peaks are not fully resolved (Figure 3). The Wild Rice cores have maximum flux of 63 μg $m^{-2}y^{-1}$ which is similar to typical forest soils. The Silver Maple soils, in contrast, have maximum flux of 167 μg $m^{-2}y^{-1}$ which far exceeds expectation for upland forest soils. The total inventory of Hg in the soils mirrors the pattern in Hg fluxes (Table 2), with lakes holding on the order of 3 mg m^{-2} (Taylor et al., 2022), peat recording ca. 4 mg m^{-2} (this study), typical forest soils averaging 8 mg m^{-2} (Landis et al., 2024a),

and Silver Maple floodplain forest accumulation over 20 mg m^{-2} of anthropogenic Hg over the past two centuries.

Across sites, the highest Hg concentrations of Hg in the Pitch Pine bog, though these cores also show the lowest Hg fluxes (Figure 3, Supplementary Figure S3; Supplementary Table S1). This underlines the importance of assessing Hg flux, not concentration, to compare Hg accumulation across sites. Unlike soil, peat is widely studied as an archive of atmospheric metal deposition (e.g., (Cooke et al., 2020)). However, the reliability of peat cores as archives of atmospheric deposition has been questioned (Biester et al., 2007; Bindler, 2006; Cooke et al., 2020), due to the potential for vertical migration or downwashing of ^{210}Pb during wetting (Biester et al., 2007; Branfireun and Roulet, 2002). In other cases, peat records are well-corroborated by other techniques (Biester et al., 2007). Here, bomb pulse ages and radionuclide inventories suggest the peat cores provides a reasonable record of accumulation (Table 2).

Within the Pitch Pine bog, the Peat core evidenced substantially lower Hg flux than the overlying Huckleberry and Pitch Pine soils. This may be in part due to lateral input of particle-bound Hg to the soils overlain by vegetation, as is inferred from the high ^{210}Pb inventory of the Pitch Pine soil. Elsewhere, peat in open areas has similarly been found to have lower Hg inventories than adjacent soils with overlying vegetation (Rydberg et al., 2015), which we attribute to higher Hg sequestration in vascular plants due to direct uptake of GEM. At the same time, higher rates of Hg evasion may also occur in open areas (Jiskra et al., 2015; Landis et al., 2024b; Li et al., 2023; Rydberg et al., 2015), and some peat cores may also be prone to Hg losses via leaching (Branfireun and Roulet, 2002). When compared to other records, peat cores have been reported to have lower pre-anthropogenic Hg fluxes, but anthropogenic enrichment factors can vary across sites which makes these comparisons challenging (Biester et al., 2007; Bindler, 2006; Cooke et al., 2020). The low Hg flux in peat is suggested to be due to receiving Hg primarily from wet deposition (Guédron et al., 2018; Lamborg et al., 2002), though Hg isotope studies have revealed peat to also accumulate Hg via dry deposition (Enrico et al., 2016). Here, the reconstruction of consistent Hg flux histories between peat and other bog soils suggests that the Missisquoi peat core does provide an accurate history of Hg deposition, but one that reflects low rates of Hg accumulation. The much higher fluxes to other Pitch Pine and Silver Maple forest soils underscores the importance of GEM deposition to high Hg accumulation in forested ecosystems (Obrist et al., 2021).

The anthropogenic Hg flux recorded in the Silver Maple floodplain is higher than any other site. Flux to the Silver Maple soils was over twice what we observed in the Pitch Pine soil, both under mature forest canopy, though this is not unexpected due to the potential for both river and canopy foliar Hg inputs to this site. The much higher anthropogenic Hg flux to the Silver Maple versus Wild Rice soil is unexpected. In river floodplains, radionuclide inventories have been used to estimate the amount of overbank deposition (He and Walling, 1996; Renshaw et al., 2014; Walling and He, 1993). In this study, similar ^{210}Pb inventories, much higher than expected from regional atmospheric deposition alone, were observed in the adjacent Silver Maple and Wild Rice soils (Table 2), suggesting comparable inputs of particle-bound metals from the river to both sites. Overlying foliar production (above-ground primary productivity) estimated from the LRC model in the rice marsh is also comparable (0.9 kg $m^{-2}y^{-1}$) to what we estimate from Oi horizon of the Silver Maple forest (0.8 kg $m^{-2}y^{-1}$, not accounting for decomposition of the prior 6 months since leaf fall). This suggests that GEM deposition should be similar between the Silver Maple and Wild Rice if it is tied to net primary productivity and foliar GEM assimilation. The Wild Rice soil shows substantially lower Hg accumulation, however, and we therefore suggest that GEM evasion (Kwon et al., 2018) or possibly loss of Hg bound to DOM (dissolved organic matter) (Wang et al., 2020) to the lake or adjacent floodplain are pathways in the Hg cycle of the Wild Rice marsh.

Despite the dynamic nature of delta environments, diverse delta soils are all shown to retain Hg over time scales of 1-2 centuries, and to capture reliable records of Hg accumulation. The apportioning of Hg input pathways to each region of the delta are discussed in detail below.

4.2 Depositional pathways of Hg across soils within the delta

To examine Hg accumulation from atmosphere and watershed sources across natural communities in the delta, total Hg accumulation rates were averaged over the past 10 years, from 2014 to 2024 (Figure 4; values also in Supplementary Table S2) for each site. Pathways of Hg accumulation were then assessed as follows, i) reconstruction of Hg flux from foliar uptake, ii) regional records of Hg wet deposition, and iii) estimates of watershed-sourced atmospheric metals based on radionuclide inventory mass balance. In addition, previous assessments of Hg deposition pathways to forest soils (without riverine inputs) provide reference values for northeastern forests, including the following: foliar GEM (12 μg $m^{-2}y^{-1}$); non-foliar GEM (12–20 μg $m^{-2}y^{-1}$), which includes deposition to forest floor, soil surfaces, and non-foliar canopy surfaces; direct wet deposition (7 μg $m^{-2}y^{-1}$); and minor contributions from dry deposition of Hg^{2+} and particulate-bound Hg (Obrist et al., 2021; Zhou et al., 2023). These sum to an estimated 22–33 μg $m^{-2}y^{-1}$ for total atmospheric Hg flux to coniferous and deciduous forest ecosystems (Obrist et al., 2021; Zhou et al., 2023), and have been verified against independent soil Hg accumulation rates (Landis et al., 2024a).

For Missisquoi delta soils, wet deposition of Hg was confirmed from precipitation records from a nearby Mercury Deposition Network (MDN) station in Underhill, VT to be 7.1 μg $m^{-2}y^{-1}$ over the past 10 years (NADP, 2024). The three Pitch Pine bog soils exhibited a broad range of recent Hg fluxes, with Peat having a mean flux of 14 μg $m^{-2}y^{-1}$, whereas mean fluxes to the Huckleberry and Pitch Pine soils (39 μg $m^{-2}y^{-1}$ and 34 μg $m^{-2}y^{-1}$, respectively) were more than twice as high. These sites are distant from the river, and rarely flooded, and we consider them to have no watershed input. Furthermore, inventories of $^{210}Pb_{ex}$ and the bomb pulse radionuclides in the Peat core are in close agreement with predicted regional fluxes at this site (Table 2), which suggests radionuclides, and by proxy, Hg, accumulate in peat strictly by direct deposition. For the Peat core, which had no overlying vegetation and therefore no foliar GEM uptake, we assume that dry deposition of Hg occurs only via the "non-foliar" pathways; this

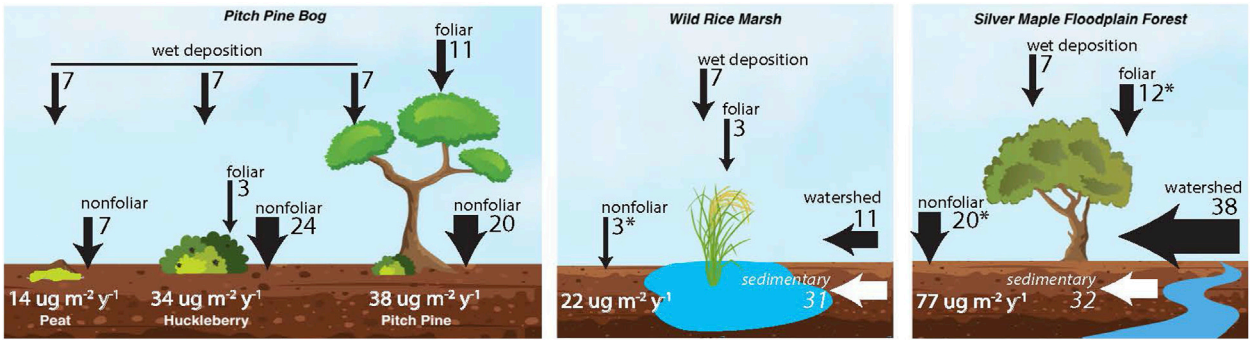

FIGURE 4
Source apportionment of Hg deposition to natural communities in the Missisquoi River delta, **(A)** Sphagnum peat, huckleberry shrub, and pitch pine forest of the Pitch Pine Bog. **(B)** Wild Rice marsh. **(C)** Silver Maple floodplain. Fluxes are shown in black arrows with unit ug $m^{-2}y^{-1}$. Average total soil accumulation rates for 2014–2024 are indicated in white text. Geogenic sedimentary inputs (italics) are not included in flux totals. Asterix indicate values estimated from literature.

was estimated as 7 μg $m^{-2}y^{-1}$, calculated as the difference between the total Hg flux measured in the core and that attributed to wet deposition (7 μg $m^{-2}y^{-1}$). The estimate of 7 μg $m^{-2}y^{-1}$ Hg from dry deposition is lower than that estimated by mass balance in a high-altitude peat bog in France, though we note that total Hg flux was much higher at that site (34 ± 8 μg $m^{-2}y^{-1}$) (Enrico et al., 2016).

Much higher Hg fluxes in the Huckleberry and Pitch Pine soils (34 and 38 μg $m^{-2}y^{-1}$, respectively) are attributable both to foliar GEM deposition, and more so to non-foliar GEM accumulation. Overlying the Huckleberry soil was a dense canopy of huckleberry shrubs, having a dry mass of foliage totalling 0.4 kg m^{-2}. The corresponding foliar Hg flux, calculated from Hg concentrations, dry mass and LRC age of the huckleberry foliage, was 3 μg $m^{-2}y^{-1}$, which reaches the soil through litterfall. Non-foliar deposition, which is a combination of dry GEM surface sorption and throughfall in this core, is estimated by mass balance as the reconstructed soil accumulation rate, minus both wet deposition and foliar uptake. This difference (24 μg $m^{-2}y^{-1}$) is much higher than in the Peat core but readily attributable to high surface area of the overlying vegetation and soil litter layer driving higher GEM sorption (e.g., (Zhou et al., 2023). We measured 10 μg $m^{-2}y^{-1}$ Hg accumulated on twigs and branches of the huckleberry shrubs with foliage removed, which supports the high rate of surface Hg sorption in this dense overlying vegetation.

In the Pitch Pine soil, an understory of huckleberry foliage (0.6 kg m^{-2}) combined with pitch pine canopy (0.2 kg m^{-2} estimated from leaf area index and leaf mass area) yield a total foliar Hg deposition of 11 μg $m^{-2}y^{-1}$, which is in good agreement with the value reported for other northeastern forest canopies (11.2 and 12.3 μg $m^{-2}y^{-1}$) (Zhou et al., 2023). Non-foliar GEM deposition estimated by mass balance was 20 μg m^{-2} y^{-1}, comparable to the Huckleberry and also very similar to non-foliar flux in temperate deciduous forest soils (25 μg $m^{-2}y^{-1}$) (Obrist et al., 2021; Zhou et al., 2023). It is noted that the extrapolated ^{210}Pb inventory in the Pitch Pine was much higher than expectation for the regional reference value, and due to the lack of river influence at this site, higher ^{210}Pb (and Hg) input may also reflect lateral focusing of particle-bound metals with organic matter in the hummucky terrain. More work will be required to understand the coupling of organic matter, Hg and ^{210}Pb dynamics in the bog's hummuck-and-hollow terrain.

In both of the Long Channel environments, sedimentary inputs supply a substantial amount of Hg in geogenic form associated with alluvial silts: 32 μg $m^{-2}y^{-1}$ in the Silver Maple and 31 μg $m^{-2}y^{-1}$ in the Wild Rice. These represent 29% and 58%, respectively, of total Hg input to these environments.

Recent anthropogenic Hg (calculated following subtraction of geogenic Hg) to the Silver Maple core was 77 μg $m^{-2}y^{-1}$, which is much higher than the other delta soils. Foliar Hg deposition rates to the Silver Maple soil were adopted from an average foliar flux value for forests in the Northeast (12 μg $m^{-2}y^{-1}$, Landis et al., 2024a) due to difficulties in obtaining foliage samples from these large trees with >30 m canopy height. A typical non-foliar Hg flux of 20 μg $m^{-2}y^{-1}$ was also taken from literature (Obrist et al., 2021). The measured flux in Oi litter layer of 33 μg $m^{-2}y^{-1}$ supports these assumptions, since the Oi litter encompasses both foliar uptake in litterfall and non-foliar GEM deposition to the forest floor. After also accounting for 7 μg $m^{-2}y^{-1}$ wet deposition flux, the remaining Hg flux was attributed to watershed inputs (38 μg $m^{-2}y^{-1}$). Watershed input thus represents approximately half of the total anthropogenic Hg flux. The observed ^{210}Pb inventory at this site was ~1.4 times the expected inventory from direct deposition (Table 2), corroborating that these soils are likely sequestering ^{210}Pb and other particle-bound metals from watershed inputs. Comparison of the Hg flux profiles in the Silver Maple delta soil with those from other forested soils in the Northeast (Landis et al., 2024a) highlights the very high Hg flux to Silver Maple soils that we attribute to their proximity to the river channel (Figure 3B). Elsewhere it has been shown that atmospheric metals preferentially accumulate along channel margins above the 5-year flood mark (Gartner et al., 2023), and we posit that this effect may be especially important for accumulation of atmospheric Hg in delta enviroments.

The recent anthropogenic Hg flux to the Wild Rice was ~22 μg $m^{-2}y^{-1}$. This value is much lower than the flux to the Silver Maple Berm, and as mentioned above, there is some possibility of Hg loss in this inundated marsh prior to deposition to the soil. Foliar deposition to the Wild Rice soils was obtained from Hg analysis of rice foliage and stalk, with net foliar accumulation of 6 μg $m^{-2}y^{-1}$.

In contrast to forest trees which have been shown to take up Hg predominantly from foliage (Arnold et al., 2018), rice plants as well as salt marsh vegetation have been shown to take up Hg from their roots as well with root-shoot transfer of Hg to foliage (Kwon et al., 2018; Wang et al., 2024). Hg flux measured in the Wild Rice root biomass was nearly twice that in foliage (6 and 13 μg $m^{-2}y^{-1}$, respectively). To correct our estimated foliar uptake for the root-shoot transfer of Hg, which is ultimately re-deposited to the sediment when plants senesce, we conservatively assumed foliar Hg accumulation in the soil as half of the Hg flux to the wild rice foliage (3 μg $m^{-2}y^{-1}$). Nonfoliar Hg deposition to the rice marsh is expected to be very low due to low depositional velocity of GEM to water surfaces, and here was approximated as 3 μg $m^{-2}y^{-1}$ based on literature values of similar environments (Kwon et al., 2018; Zhang et al., 2016). After accounting for Hg flux from precipitation (7 μg $m^{-2}y^{-1}$), a remaining Hg flux of 9 μg $m^{-2}y^{-1}$ is attributed to watershed sources, representing about 50% of the total atmospheric Hg flux to the marsh soils. The inventory of ^{210}Pb in this core was also 130% of the regional average, which supports the notion of lateral input of particle bound metals from the watershed.

4.3 Implications for role of delta soils

Delta soils serve an important function in sequestering and retaining Hg, though the pathways of Hg accumulation are variable among contrasting environments. Importantly, despite being subjected to frequent hydrologic disturbance and inundation, radionuclide and Hg profiles reveal that particle-bound metals such as Hg and Pb are strongly retained within these soils over relatively long-time scales (~200 years). The reconstruction of Hg fluxes across contrasting plant communities of the delta provide insight into Hg cycling in these environments, which has not previously been possible with measurements of Hg concentrations alone. These findings emphasize the importance of delta soils as a long-term sink for Hg and therefore support the preservation of coastal deltaic and floodplain ecosystems because they serve an important ecosystem service in sequestering Hg from atmospheric and river inputs.

Plain language summary

Delta soils accumulate and store mercury from both the atmosphere and from watersheds. Comparing mercury flux to soils across different regions of a delta informs how flood frequency and vegetation cover control mercury capture and retention in these important environments.

Data availability statement

The original contributions presented in the study are included in the article/Supplementary Material, further inquiries can be directed to the corresponding author.

Author contributions

PG: Data curation, Writing–original draft. JL: Data curation, Writing–original draft, Conceptualization, Formal Analysis, Investigation, Methodology, Visualization, Writing–review and editing. TW: Writing–review and editing. VT: Writing–review and editing, Conceptualization, Data curation, Funding acquisition, Investigation, Methodology, Project administration, Resources, Supervision, Visualization, Writing–original draft.

Funding

The author(s) declare that financial support was received for the research, authorship, and/or publication of this article. We thank the Lake Champlain Basin Program for funding, and Dartmouth EARS Dept and UGAR for thesis support for PG.

Acknowledgments

We thank the Lake Champlain Basin Program for funding, and Dartmouth EARS Dept and UGAR for thesis support for PG.

Conflict of interest

The authors declare that the research was conducted in the absence of any commercial or financial relationships that could be construed as a potential conflict of interest.

Generative AI statement

The authors declare that no Generative AI was used in the creation of this manuscript.

Publisher's note

Supplementary material

The Supplementary Material for this article can be found online at: https://www.frontiersin.org/articles/10.3389/fenvc.2025.1552966/full#supplementary-material

References

Arnold, J., Gustin, M. S., and Weisberg, P. J. (2018). Evidence for nonstomatal uptake of Hg by aspen and translocation of Hg from foliage to tree rings in Austrian pine. *Environ. Sci. Technol.* 52, 1174–1182. doi:10.1021/ACS.EST.7B04468

Biester, H., Bindler, R., Martinez-Cortizas, A., and Engstrom, D. R. (2007). Modeling the past atmospheric deposition of mercury using natural archives. *Environ. Sci. Technol.* 41, 4851–4860. doi:10.1021/es0704232

Bindler, R. (2006). Mired in the past — looking to the future: geochemistry of peat and the analysis of past environmental changes. *Glob. Planet. Change* 53, 209–221. doi:10.1016/J.GLOPLACHA.2006.03.004

Branfireun, B. A., and Roulet, N. T. (2002). Controls on the fate and transport of methylmercury in a boreal headwater catchment, northwestern Ontario, Canada. *Hydrol. Earth Syst. Sci.* 6, 785–794. doi:10.5194/hess-6-785-2002

Clews, C. (2002). From floodplain forest to pitch pine woodland bog, A landscape inventory and analysis of the Missisquoi national Wildlife Refuge, Swanton, Vermont. Master's thesis University of Vermont.

Cooke, C. A., Martínez-Cortizas, A., Bindler, R., and Sexauer Gustin, M. (2020). Environmental archives of atmospheric Hg deposition – a review. *Sci. Total Environ.* 709, 134800. doi:10.1016/j.scitotenv.2019.134800

Demers, J. D., Blum, J. D., and Zak, D. R. (2013). Mercury isotopes in a forested ecosystem: implications for air-surface exchange dynamics and the global mercury cycle. *Glob. Biogeochem. Cycles* 27, 222–238. doi:10.1002/gbc.20021

Demers, J. D., Sherman, L. S., Blum, J. D., Marsik, F. J., and Dvonch, J. T. (2015). Coupling atmospheric mercury isotope ratios and meteorology to identify sources of mercury impacting a coastal urban-industrial region near Pensacola, Florida, USA. *Glob. Biogeochem. Cycles* 29, 1689–1705. doi:10.1002/2015GB005146

Driscoll, C. T., Han, Y. J., Chen, C. Y., Evers, D. C., Lambert, K. F., Holsen, T. M., et al. (2007). Mercury contamination in forest and freshwater ecosystems in the northeastern United States. *Bioscience* 57, 17–28. doi:10.1641/B570106

Enrico, M., Roux, G. L., Marusczak, N., Heimbürger, L. E., Claustres, A., Fu, X., et al. (2016). Atmospheric mercury transfer to peat bogs dominated by gaseous elemental mercury dry deposition. *Environ. Sci. Technol.* 50, 2405–2412. doi:10.1021/acs.est.5b06058

Gartner, J. D., Renshaw, C. E., Landis, J., and Magilligan, F. J. (2023). Impact of stream power gradients on storage of sediment and carbon on channel margins and floodplains. *Geology* 51, 13–17. doi:10.1130/G50339.1

Guédron, S., Ledru, M. P., Escobar-Torrez, K., Develle, A. L., and Brisset, E. (2018). Enhanced mercury deposition by Amazonian orographic precipitation: evidence from high-elevation Holocene records of the Lake Titicaca region (Bolivia). *Palaeogeogr. Palaeoclimatol. Palaeoecol.* 511, 577–587. doi:10.1016/j.palaeo.2018.09.023

He, Q., and Walling, D. E. (1996). Use of fallout Pb-210 measurements to investigate longer-term rates and patterns of overbank sediment deposition on the floodplains of lowland rivers. *Earth Surface Processes Landforms*. 21, 141–154.

Jiskra, M., Wiederhold, J. G., Skyllberg, U., Kronberg, R. M., Hajdas, I., and Kretzschmar, R. (2015). Mercury deposition and Re-emission pathways in boreal forest soils investigated with Hg isotope signatures. *Environ. Sci. Technol.* 49, 7188–7196. doi:10.1021/acs.est.5b00742

Kaste, J. M., Volante, P., and Elmore, A. J. (2021). Bomb 137Cs in modern honey reveals a regional soil control on pollutant cycling by plants. *Nat. Commun.* 121 (12), 1937–7. doi:10.1038/s41467-021-22081-8

Kwon, S. Y., Selin, N. E., Giang, A., Karplus, V. J., and Zhang, D. (2018). Present and future mercury concentrations in Chinese rice: insights from modeling. *Glob. Biogeochem. Cycles* 32, 437–462. doi:10.1002/2017GB005824

Lamborg, C. H., Fitzgerald, W. F., Damman, A. W. H., Benoit, J. M., Balcom, P. H., and Engstrom, D. R. (2002). Modern and historic atmospheric mercury fluxes in both hemispheres: global and regional mercury cycling implications. *Glob. Biogeochem. Cycles* 16, 51–1. doi:10.1029/2001gb001847

Landis, J. D., Obrist, D., Zhou, J., Renshaw, C. E., McDowell, W. H., Nytch, C. J., et al. (2024a). Quantifying soil accumulation of atmospheric mercury using fallout radionuclide chronometry. *Nat. Commun.* 151, 5430–5511. doi:10.1038/s41467-024-49789-7

Landis, J. D., Renshaw, C. E., and Kaste, J. M. (2016). Beryllium-7 and lead-210 chronometry of modern soil processes: the Linked Radionuclide aCcumulation model, LRC. *LRC. Geochim. Cosmochim. Acta* 180, 109–125. doi:10.1016/j.gca.2016.02.013

Landis, J. D., Renshaw, C. E., Kaste, J. M., and Blum, J. D. (2012). Measurement of 7 Be in soils and sediments by gamma spectroscopy. *Chem. Geol.* 291, 175–185. doi:10.1016/j.chemgeo.2011.10.007

Landis, J. D., Taylor, V. F., Hintelmann, H., and Hrenchuk, L. E. (2024b). Predicting behavior and fate of atmospheric mercury in soils: age-dating METAALICUS Hg isotope spikes with fallout radionuclide chronometry. *Environ. Sci. Technol.* 58, 20009–20018. doi:10.1021/ACS.EST.4C01544

Li, C., Jiskra, M., Nilsson, M. B., Osterwalder, S., Zhu, W., Mauquoy, D., et al. (2023). Mercury deposition and redox transformation processes in peatland constrained by mercury stable isotopes. *Nat. Commun.* 141 (14), 7389–7412. doi:10.1038/s41467-023-43164-8

Liu, P., Wu, Q., Wang, X., Hu, W., Liu, X., Tian, K., et al. (2022). Spatiotemporal variation and sources of soil heavy metals along the lower reaches of Yangtze River, China. *Chemosphere* 291, 132768. doi:10.1016/j.chemosphere.2021.132768

NADP (2024). *Site MDN AB08*. National Atmospheric Deposition Program. Available online at: http://nadp.slh.wisc.edu/data/mdn/ (Accessed January 15, 2024).

Obrist, D., Kirk, J. L., Zhang, L., Sunderland, E. M., Jiskra, M., and Selin, N. E. (2018). A review of global environmental mercury processes in response to human and natural perturbations: changes of emissions, climate, and land use. *Ambio* 47, 116–140. doi:10.1007/s13280-017-1004-9

Obrist, D., Roy, E. M., Harrison, J. L., Kwong, C. F., William Munger, J., Moosmüller, H., et al. (2021). Previously unaccounted atmospheric mercury deposition in a midlatitude deciduous forest. *Proc. Natl. Acad. Sci. U. S. A.* 118, e2105477118. doi:10.1073/pnas.2105477118

Perry, E., Norton, S. A., Kamman, N. C., Lorey, P. M., and Driscoll, C. T. (2005). Deconstruction of historic mercury accumulation in lake sediments, northeastern United States. *Ecotoxicology* 14, 85–99. doi:10.1007/s10646-004-6261-2

Renshaw, C. E., Abengoza, K., Magilligan, F. J., Dade, W. B., and Landis, J. D. (2014). Impact of flow regulation on near-channel floodplain sedimentation. *Geomorphology* 205, 120–127. doi:10.1016/j.geomorph.2013.03.009

Roberts, S. L., Kirk, J. L., Muir, D. C. G., Wiklund, J. A., Evans, M. S., Gleason, A., et al. (2021). Quantification of spatial and temporal trends in atmospheric mercury deposition across Canada over the past 30 years. *Environ. Sci. Technol.* 55, 15766–15775. doi:10.1021/acs.est.1c04034

Rydberg, J., Rösch, M., Heinz, E., and Biester, H. (2015). Influence of catchment vegetation on mercury accumulation in lake sediments from a long-term perspective. *Sci. Total Environ.* 538, 896–904. doi:10.1016/j.scitotenv.2015.08.133

Shanley, J. B., and Chalmers, A. T. (2012). Streamwater fluxes of total mercury and methylmercury into and out of Lake Champlain. *Environ. Pollut.* 161, 311–320. doi:10.1016/j.envpol.2011.07.006

Taylor, V. F., Landis, J. D., and Janssen, S. E. (2022). Tracing the sources and depositional history of mercury to coastal northeastern U.S. lakes. *Environ. Sci. Process. Impacts* 24, 1805–1820. doi:10.1039/d2em00214k

Walling, D. E., and He, Q. (1993). Use of cesium-137 as a tracer in the study of rates and patterns of floodplain sedimentation. *International Association of Hydrological Sciences* 215, 319–328.

Wang, G. P., Liu, J. S., and Tang, J. (2004). Historical variation of heavy metals with respect to different chemical forms in recent sediments from xianghai wetlands, northeast China. *Wetlands* 24, 608–619. doi:10.1672/0277-5212(2004)024[0608:HVOHMW]2.0.CO;2

Wang, T., Driscoll, C. T., Hwang, K., Chandler, D., and Montesdeoca, M. (2020). Total and methylmercury concentrations in ground and surface waters in natural and restored freshwater wetlands in northern New York. *Ecotoxicology* 29, 1602–1613. doi:10.1007/s10646-019-02155-6

Wang, T., Du, B., Forbrich, I., Zhou, J., Polen, J., Sunderland, E. M., et al. (2024). Above- and belowground plant mercury dynamics in a salt marsh estuary in Massachusetts, USA. *Biogeosciences* 21, 1461–1476. doi:10.5194/BG-21-1461-2024

Yuan, W., Sommar, J., Lin, C. J., Wang, X., Li, K., Liu, Y., et al. (2019). Stable isotope evidence shows Re-emission of elemental mercury vapor occurring after reductive loss from foliage. *Environ. Sci. Technol.* 53, 651–660. doi:10.1021/acs.est.8b04865

Yuan, W., Wang, X., Lin, C. J., Sommar, J. O., Wang, B., Lu, Z., et al. (2021). Quantification of atmospheric mercury deposition to and legacy Re-emission from a subtropical forest floor by mercury isotopes. *Environ. Sci. Technol.* 55, 12352–12361. doi:10.1021/ACS.EST.1C02744

Yuan, W., Wang, X., Lin, C. J., Song, Q., Zhang, H., Wu, F., et al. (2023). Deposition and Re-emission of atmospheric elemental mercury over the tropical forest floor. *Environ. Sci. Technol.* 57, 10686–10695. doi:10.1021/ACS.EST.3C01222

Zhang, H., Li, Y., Luo, Y., and Christie, P. (2015). Anthropogenic mercury sequestration in different soil types on the southeast coast of China. *J. Soils Sediments* 15, 962–971. doi:10.1007/s11368-015-1062-1

Zhang, L., Wu, Z., Cheng, I., Paige Wright, L., Olson, M. L., Gay, D. A., et al. (2016). The estimated six-year mercury dry deposition across North America. *Environ. Sci. Technol.* 50, 12864–12873. doi:10.1021/acs.est.6b04276

Zhou, J., Bollen, S. W., Roy, E. M., Hollinger, D. Y., Wang, T., Lee, J. T., et al. (2023). Comparing ecosystem gaseous elemental mercury fluxes over a deciduous and coniferous forest. *Nat. Commun.* 141 14, 2722–2729. doi:10.1038/s41467-023-38225-x